Supporting Information for

The supramolecular polymer complexes with oppositely charged calixresorcinarene: the hydrophobic domains formation and the synergistic binding mode

Julia E. Morozova [a, b,*], Victor V. Syakaev [a], Yana V. Shalaeva [a, b], Alina M. Ermakova [a, b], Irek R. Nizameev [a, c], Marsil K. Kadirov [a], Ella Kh. Kazakova [a], Alexander I. Konovalov [a]

[a]*A. E. Arbuzov Institute of Organic and Physical Chemistry, Kazan Scientific Center, Russian Academy of Science, Arbuzov str. 8, 420088 Kazan, Russian Federation*

[b]*Kazan Federal University, Kremlevskaya st. 18, 420008 Kazan, Russian Federation*

[c]*Kazan National Research Technical University, K. Marx str. 10, 420111 Kazan, Russian Federation*

*E-mail: ernestina34@gmail.com

Table of Contents

Table S1. pH-values of 1 mM solutions of carboxycalixresorcinarenes in an aqueous solution; self-diffusion coefficients (D_s), hydrodynamic radius (R_H), and aggregation numbers (N_{ag}) of macrocycles in D_2O solutions (1 mM) from NMR FT-PGSE experiments

Macrocycle	pH	$D_s \times 10^{-10}$, m^2/s	R_H, Å		N_{ag}
			exp	*teor*[a]	
C_1OPh-CR	8.04	2.55[b,c]	10.9	8.4	2.2[d]
C_5OPh-CR	8.08	2.06	13.5	9.7	2.7
C_5-CR	7.86	2.49[b]	11.2	8.6	2.2
C_8-CR	7.97	1.85[b]	15.0	9.1	4.5
C_{11}-CR	8.10	1.04[b]	26.7	9.5	22

a - the value of R_H^{teor} was estimated with the help of HYDRONMR program [1]; b - the data from ref [2]; c - C(C_1OPh-CR) = 0.5 mM; d - The aggregation numbers of calixresorcinarenes N_{ag} were estimated as described in ref [3]: $N_{ag} = (R_H^{agr}/R_H^{mon})^3$, where R_H^{agr} and R_H^{mon} are hydrodynamic radii of the molecules in aggregated and monomeric states, $R_H^{mon} = R_H^{teor}$.

Table S2. pH-values, the values of averaged hydrodynamic diameters of particles (d, nm), their intensities of scattering (I, %), and polydispersity index (PDI) in individual PEI solutions and in the presence of C_n-CR (1 mM).

Macrocycle	C(PEI), mM	d_1, nm (I_1, %)	d_2, nm (I_2, %)	PDI	ξ, mV	pH
-	0.5	16 (2.6)	106 (17.5)	0.284	+33.0	9.65
	1	18 (3.7)	91 (22.2)	0.312	+22.2	9.53
	5	24 (2.8)	106 (16.8)	0.32	+15.1	10.59
	10	28 (3.0)	106 (13.8)	0.399	+14.9	10.35
	20	21 (2.4)	106 (12.8)	0.461	+13.2	10.83
C_1OPh-CR	0.5	-	220 (39.8)	0.007	-23.0	10.44
	1	-	295 (31.1)	0.159	-17.0	10.72
	5	28 (5.9)	106 (16)	0.288	-12.7	10.49
	10	21 (3.4)	91 (15.1)	0.286	-10.3	11.09
	20	28 (5.7)	106 (14)	0.313	-7.6	11.26
C_5OPh-CR	0.5	28 (7.5)	68 (12.9)	0.203	-44.1	10.78
	1	-	37 (15)	0.151	-29.7	11.21
	5	24 (2.7)	78 (16.7)	0.165	-19.1	10.87
	10	16 (1.8)	79 (11.9)	0.278	-15.0	11.65
	20	14 (2.1)	79 (10.3)	0.302	-12.6	11.59
C_5-CR	0.5	-	58 (13.7)	0.15	-55.6	10.78
	1	-	58 (20.4)	0.089	-34.5	11.11
	5	21 (3.9)	91 (18)	0.283	-21.7	10.77
	10	12 (3.1)	79 (14.1)	0.288	-15.3	11.52
	20	24 (3.3)	91 (14.5)	0.376	-10.2	11.55
C_8-CR	0.5	18 (2.1)	58 (14.3)	0.186	-55.5	11.39
	1	-	68 (14.6)	0.182	-46.7	11.39
	5	24 (3.6)	91 (12.7)	0.295	-27.3	11.00
	10	18 (2.6)	91 (14.5)	0.300	-22.5	11.86
	20	16 (2.2)	91 (14.4)	0.310	-13.7	11.65
C_{11}-CR	0.5	-	78 (14.3)	0.192	0	10.92
	1	-	68 (14.1)	0.228	0	11.37
	5	18 (3.6)	78 (14.3)	0.277	0	10.94
	10	14 (2.4)	68 (13.8)	0.251	0	11.13
	20	18 (4.3)	91 (14.6)	0.311	0	11.59
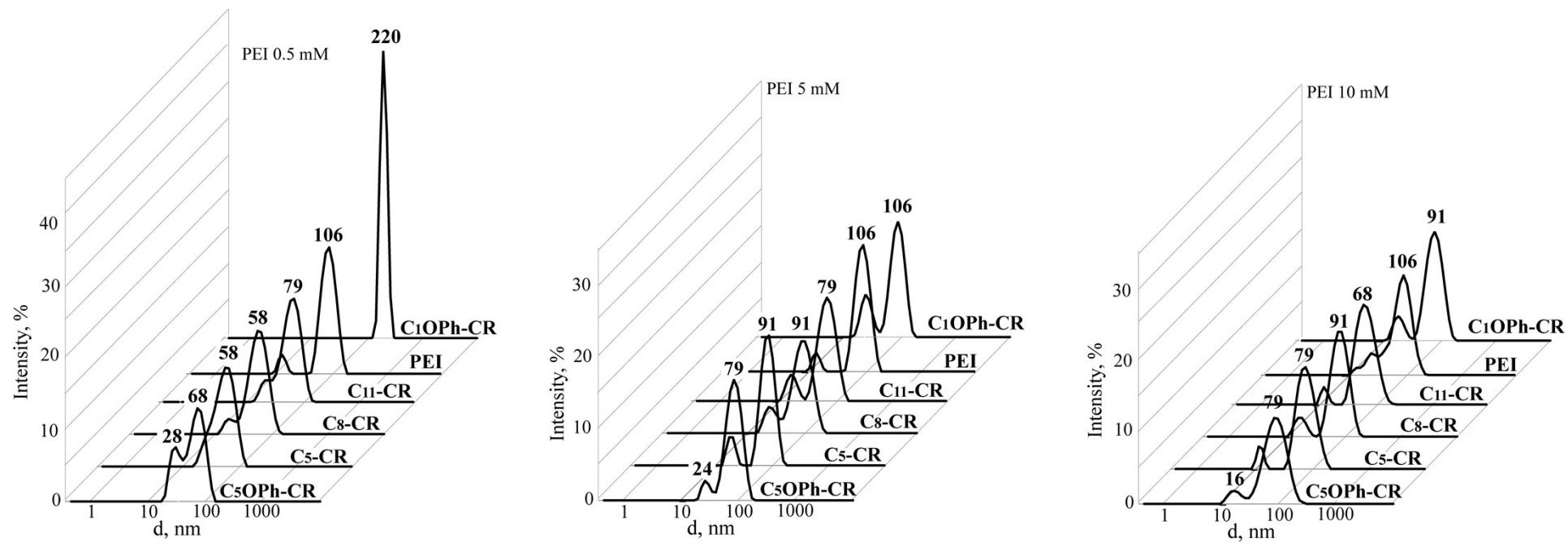
Figure S1. The intensity-averaged size distribution for PEI and PEI - C_n-CR solutions (DLS method, 25 °C, C(C_n-CR) 1 mM, C(PEI) 0.5, 5 and 10 mM).

R' = CH$_2$COO$^-$

R = ⟨phenyl⟩—OCH$_3$ R = ⟨phenyl⟩—O(CH$_2$)$_4$CH$_3$

C$_5$H$_{11}$, C$_8$H$_{17}$, C$_{11}$H$_{23}$

chair   *boat*

Figure S2. The conformational structures of Cn-CR (according to H^1 NMR data [2, 4]).

a)

b)

c)

Figure S3. The I/III dependence of values of pyrene on concentration of Cn-CR in the absence and presence of 5 and 20 mM PEI: a – for C$_1$OPh-CR, b - for C$_5$OPh-CR, c - for C$_5$-CR.

Figure S4. UV VIS spectra of Orange OT after solubilization by individual and mixed solutions of PEI (a), C1OPh-CR (b), C5-CR (c), C5OPh-CR (d), C8-CR (e), C11-CR (f)

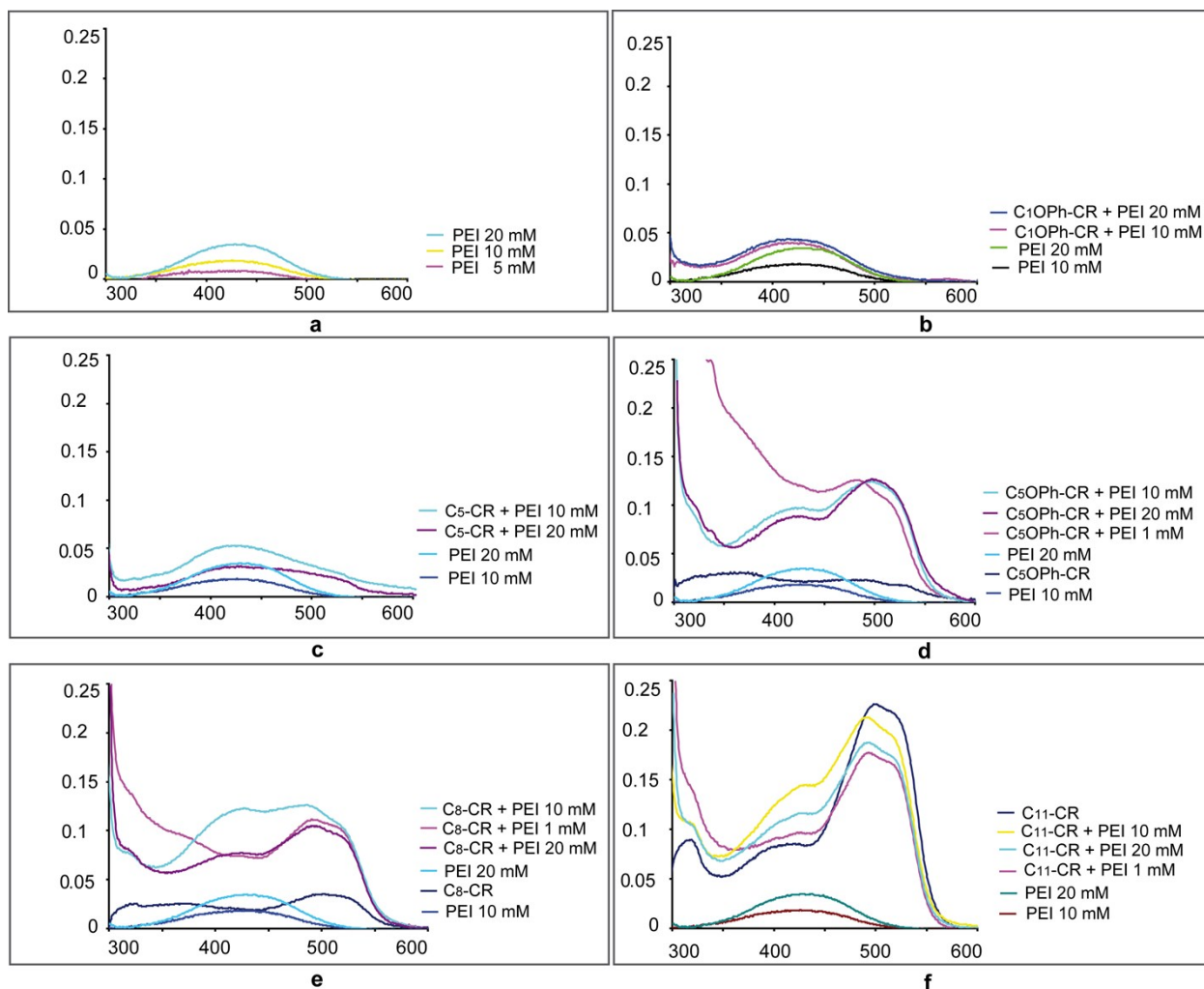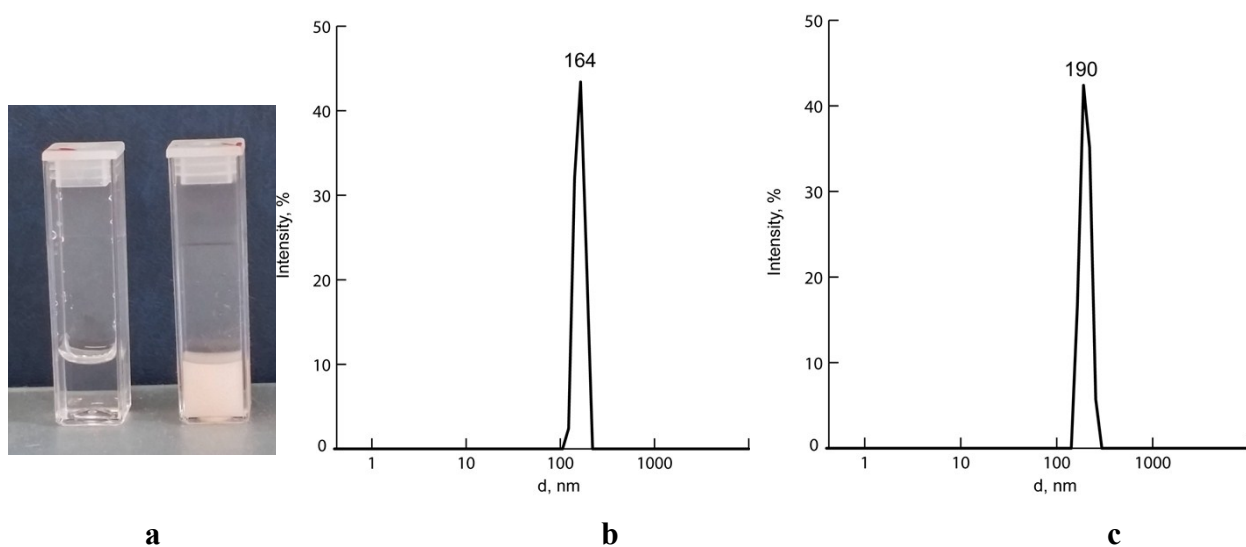**Figure S5.** a – The photo of C_8-CR - PEI (left) and C_8-CR - PEI – Orange OT (on right) solutions (C(PEI) 5 mM). b, c – The intensity-averaged size distribution for C_8-CR – PEI - Orange OT (b) and C_5OPh-CR - PEI - Orange OT (c) solutions (C(PEI) 5 mM).
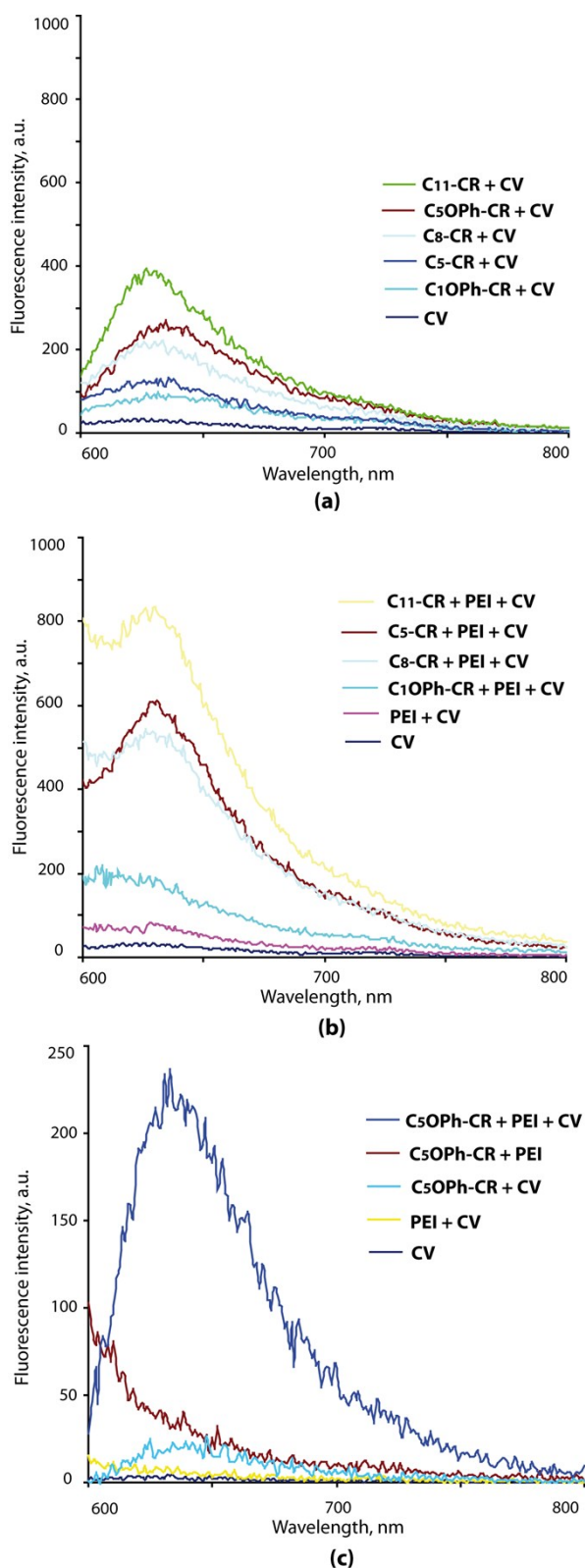
Figure S6. Emission spectra of CV (0.001 mM) in individual solution and in the individual and mixed solutions of Cn-CR (1 mM) and PEI (5 mM); λ_{ex} 580 nm, voltage 800V, (a) and (b) - ex.slit 10 nm, em.slit 10 nm; (c) - ex.slit 5 nm, em.slit 5 nm, the spectrum of C5OPh-CR - PEI solution is added as a blank because a weakly fluorescent "background" from PEI was observed. The emission maximum of CV (633 nm) is shifted to 628 nm in the presence of tetra-alkyl macrocycles C_5-CR, C_8-CR, and C_{11}-CR and to 635 nm in the presence of tetra-phenylenoxyalkyl macrocycles C_1OPh-CR and C_5OPh-CR due to the binding. Probably, this difference between observed shifts occurs due to the binding of the dye near the phenylenoxy groups of macrocycles in the last case.

Table S3. The NMR FT-PGSE data for PEI[a] and C_5-CR and C_5OPh-CR (D_2O, 303 K): D_s - the self-diffusion coefficient of macrocycle, P_b - fraction of macrocycle bound by PEI, D_s^{fast}, D_s^{slow}, P^{fast}, and P^{slow} - the self-diffusion coefficient and the population for fast and slow components in two exponential analyses of PEI diffusion slope, respectively; D_s^P– the population weighted average of the diffusion coefficients of PEI; $R_H$fast/slow - experimental value of hydrodynamic radius of fast and slow components of PEI, respectively; C_{Cn-CR} 1 mM.

Cn-CR	C(PEI), mM	$D_s\times10^{-10}$, m²/s Cn-CR	$D_s\times10^{-10}$, m²/s (P) PEI fast	slow	$D_s^P\times10^{-10}$, m²/s PEI	$R_H$fast/slow, A PEI	P_b Cn-CR
PEI	5	-	1.59 (0.40)	0.21 (0.60)	0.75	18 / ~135	-
C_5-CR	0	2.49	-	-	-	-	-
	0.25	2.47	b	b	-	-	-
	2.5	1.96	1.53 (0.73)	0.25 (0.27)	1.19	18 / 110	0.49
	5	1.81	1.43 (0.63)	0.25 (0.37)	0.99	20 / 110	0.52
	10	1.39	1.72 (0.45)	0.25 (0.55)	0.91	16 / 110	0.73
	20	1.03	1.65 (0.43)	0.26 (0.57)	0.85	17 / 110	0.90
C_5OPh-CR	0	2.06	-	-	-	-	-
	0.25	2.03	b	b	-	-	-
	0.5	2.08	b	b	-	-	-
	0.75	2.08	b	b	-	-	-
	1	2.06	b	b	-	-	-
	2.5	1.96	1.65 (0.53)	0.25 (0.47)	0.99	17 / 110	0.10
	5	1.87	1.65 (0.74)	0.28 (0.26)	1.29	17 / 100	0.24
	10	1.26	1.90 (0.47)	0.29 (0.53)	1.04	15 / 100	0.78
	20	0.89	1.73 (0.53)	0.26 (0.47)	1.05	16 / 105	1.16[c]

a - The concentration of PEI is per monomer unit in all case; b - the short times of transverse relaxation T2* for polymer signals are observed that don't allow to estimate PEI self-diffusion coefficient; c - the macrocycle is bound by slow component of PEI, that leads to the overestimation of its P_b value.
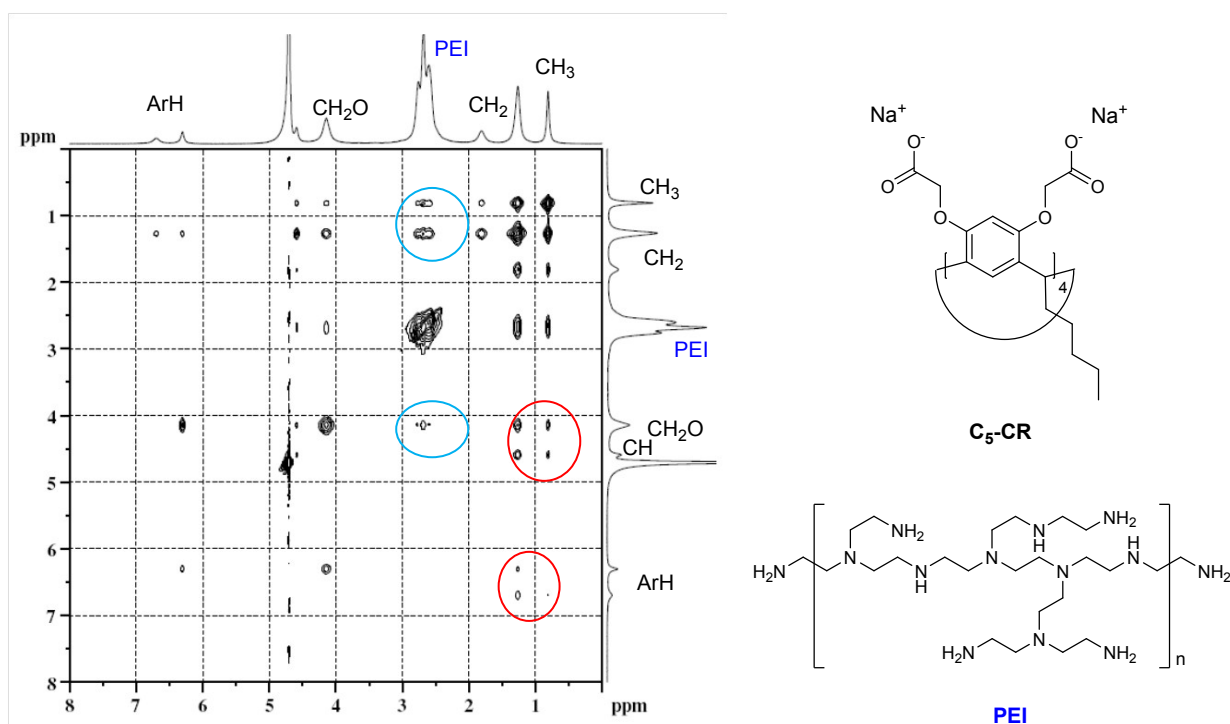
Figure S7. 2D NOESY spectrum of C_5-CR − PEI solution (C(C_5-CR) 1 mM, C(PEI) 5 mM) in D_2O, the red circle indicates the cross peaks between signals of macrocycles groups, the blue circle indicates the cross peaks between signals of groups of macrocycle and PEI.

In the 2D NOESY spectrum the cross peaks between signals of ethylene groups of PEI and hydrophilic and aliphatic groups of the macrocycle are observed in the 2D NOESY spectrum (indicated by blue circles). The closeness of CH_2O groups of the macrocycle and NCH_2CH_2N groups of PEI are occured as a result of electrostatic interaction of charged groups of components. The cross peaks between NCH_2CH_2N groups of PEI and pentyl groups of the macrocycle can mean the inclusion of PEI fragments in macrocycle dimer or enveloping of macrocycle aliphatic groups by polymer chain. The cross peaks between signals of macrocycles groups indicated by red circles can be intra- or intermolecular.
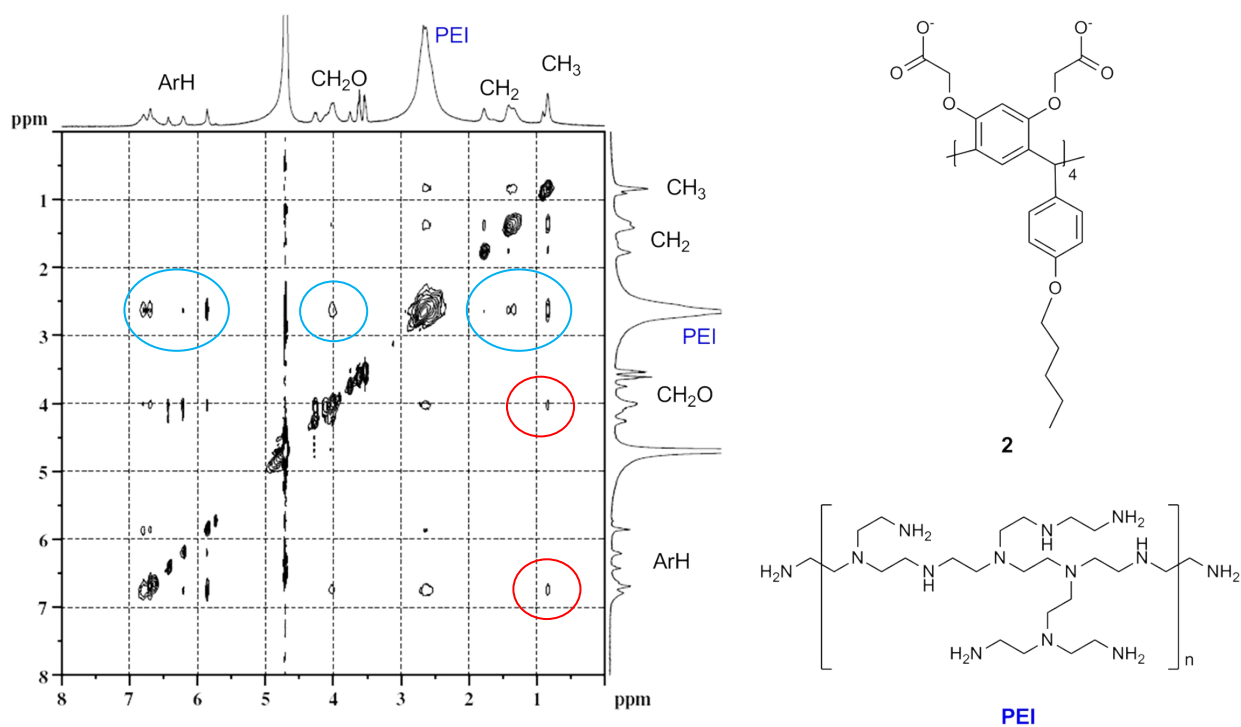
Figure S8. 2D NOESY spectrum of C_5OPh-CR − PEI solution ($C(C_5OPh$-CR) 1 mM, C(PEI) 5 mM) in D_2O, the red circle indicates the cross peaks between signals of macrocycles groups, the blue circle indicates the cross peaks between signals of groups of macrocycle and PEI.

In the 2D NOESY spectrum the cross peaks between signals of PEI fragments and aromatic, aliphatic and hydrophilic groups of the macrocycle indicated by blue circles as well as the cross peaks between signals of aromatic and aliphatic groups and hydrophilic and aliphatic groups of macrocycle molecules are observed in the 2D NOESY spectrum.
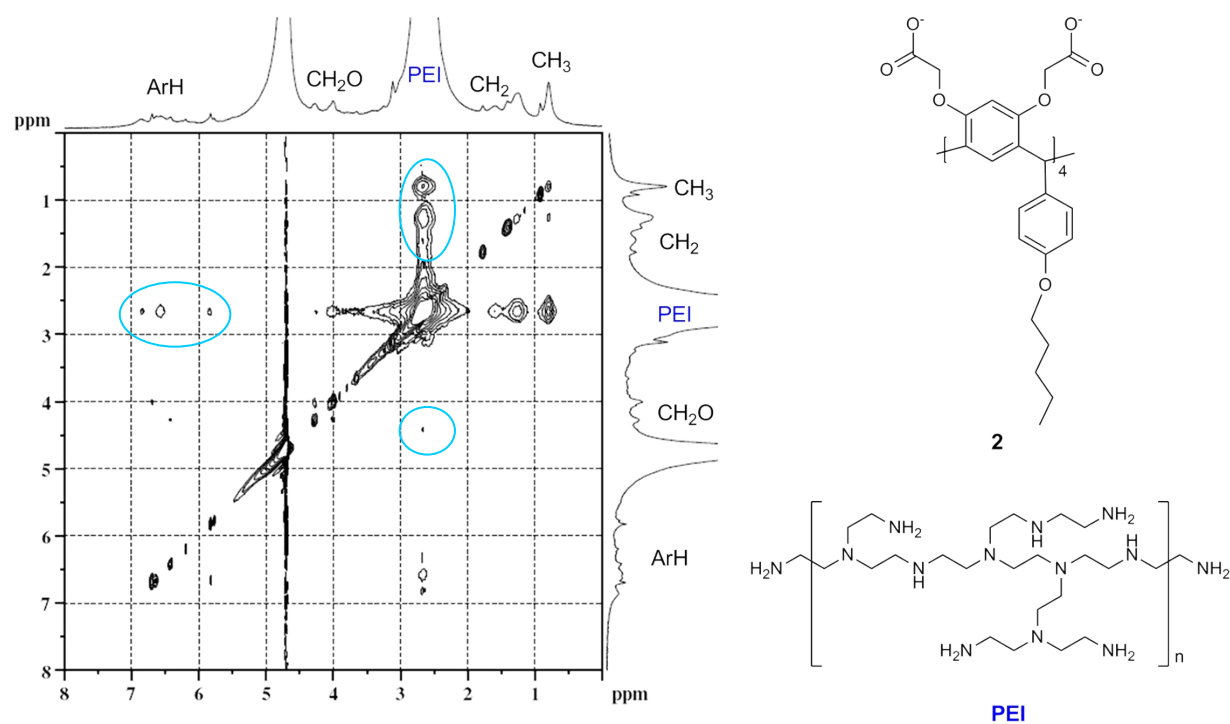
Figure S9. 2D NOESY spectrum of $C_5OPh\text{-}CR$ – PEI solution ($C(C_5OPh\text{-}CR)$ 1 mM, $C(PEI)$ 20 mM) in D_2O, the blue circle indicates the cross peaks between signals of groups of macrocycle and PEI.

The cross peaks between signals of PEI fragments and aromatic, aliphatic and hydrophilic groups of the macrocycle indicated by blue circles are observed in the 2D NOESY spectrum. The cross peaks between signals of PEI fragments and aliphatic groups of the macrocycle are very strong.
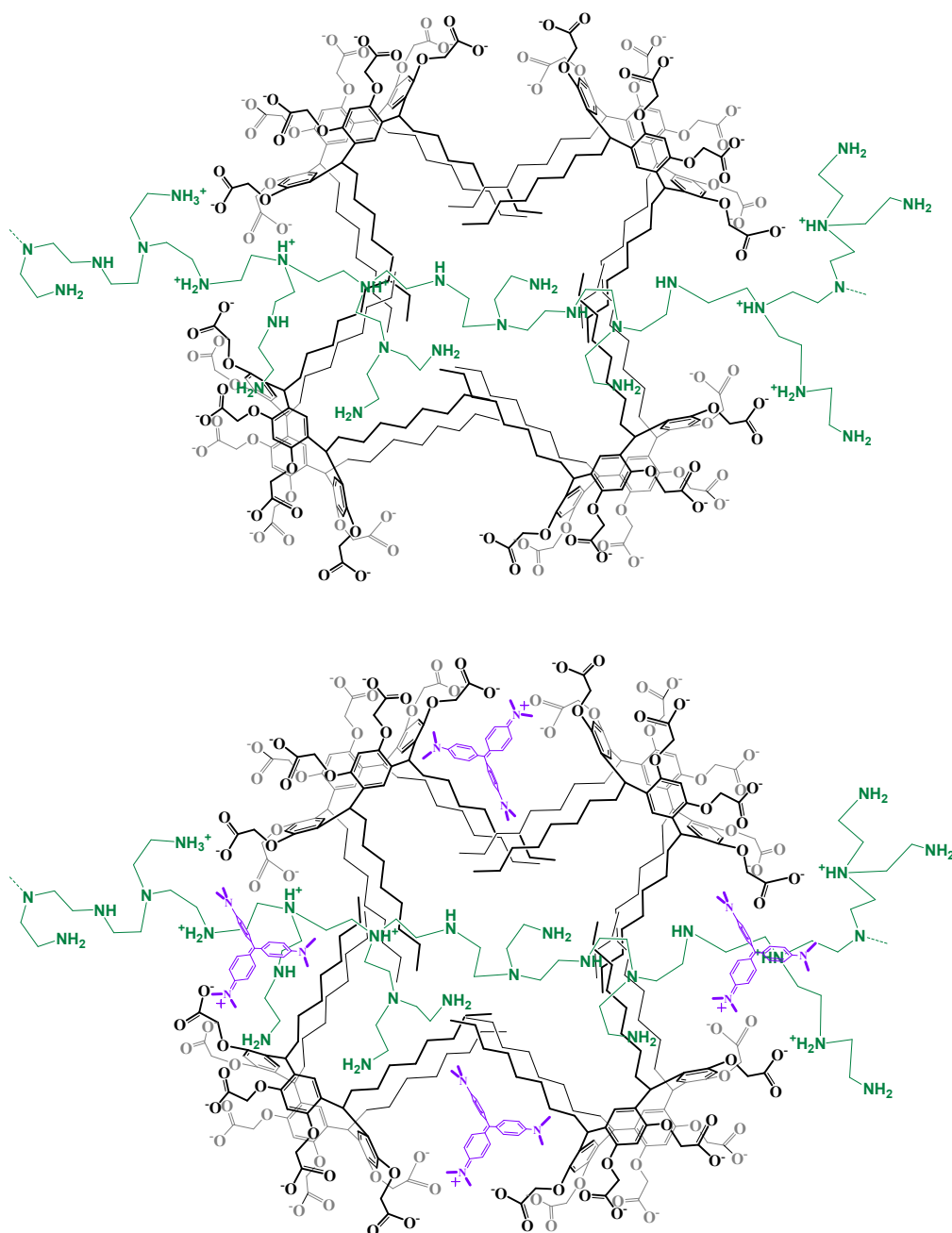
Figure S10. The proposed scheme of C_8OPh-CR + PEI (up) and C_8OPh-CR + CV + PEI (down) complexes.

In the scheme the electrostatic and hydrophobic interactions between the macrocycle and PEI as well as the increasing of CV emission as a result of partial participation of PEI in the bounding of CV are took in to the account. The inner part of complex comprises alkyl groups of macrocycle and some fragments of PEI, and the upper part is mainly composed by hydrophilic groups of macrocycle molecules.
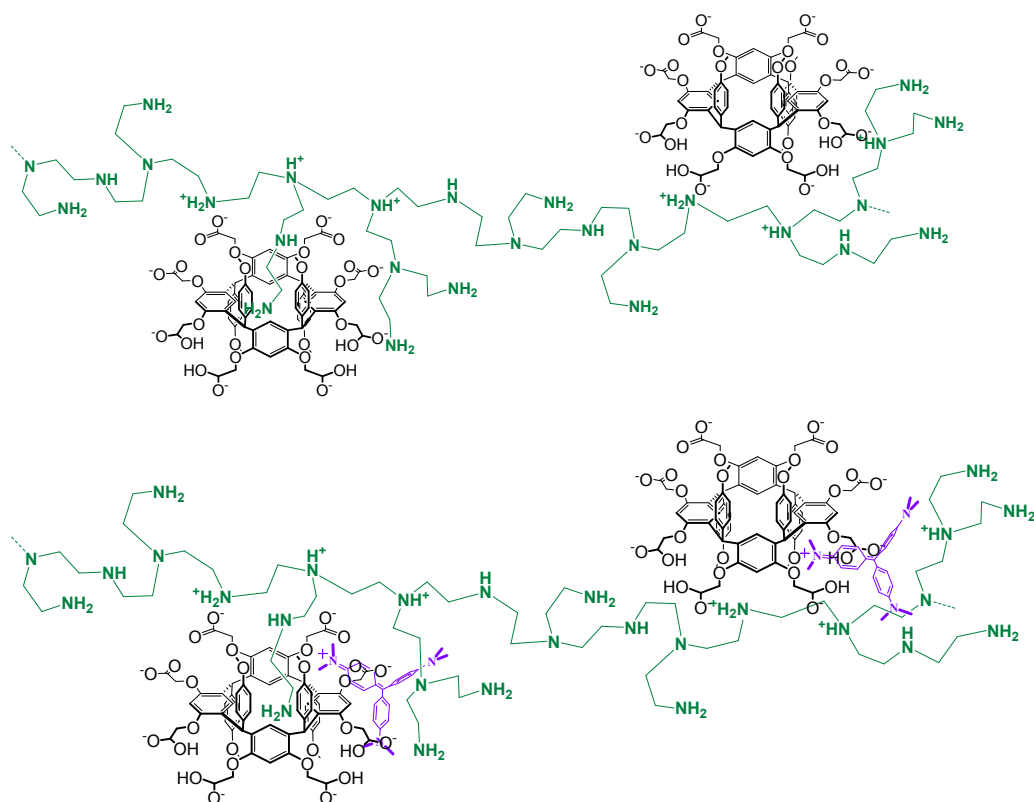
Figure S11. The proposed scheme of C_1OPh-CR + PEI (up) and C_1OPh-CR + CV + PEI (down) complexes. The molecules of C_1OPh-CR are in chair conformation.

References

1 J. G. de la Torre, M.L. Huertas, B. Carrasco, *J. Magn. Res.*, 2000, **147,** 138.

2 D. A. Mironova, L. A. Muslinkina, V. V. Syakaev, J. E. Morozova, V. V. Yanilkin, A. I. Konovalov, E. Kh. Kazakova, *J. Colloid Interface Sci.*, 2013, **407**, 148-154.

3 V. V. Syakaev, E. Kh. Kazakova, Ju. E. Morozova, Ya. V. Shalaeva, Sh. K. Latypov, A. I. Konovalov, *J. Colloid Interface Sci.*, 2012, **370**, 19-26.

4 Ju. E. Morozova, V. V. Syakaev, Ya. V. Shalaeva, A. M. Ermakova, I. R. Nizameev, M. K. Kadirov, A. D. Voloshina, V. V. Zobov, I. S. Antipin, A. I. Konovalov, *Soft Matter*, 2017, **13,** 2004-2013.